International Journal of Heat and Mass Transfer 52 (2009) 2646–2659

Contents lists available at ScienceDirect

International Journal of Heat and Mass Transfer

journal homepage: www.elsevier.com/locate/ijhmt

Analysis of thermal performance and optimization of concentric circular fins under dehumidifying conditions

B. Kundu *

Department of Mechanical Engineering, Jadavpur University, Kolkata 700 032, India

ARTICLE INFO

Article history:
Received 20 September 2007
Received in revised form 15 December 2008
Available online 24 February 2009

Keywords:
Analytical method
Annular disc fin
Annular step fin
Fin efficiency
Material saving
Optimization

ABSTRACT

The analysis of wet fins was carried out by many investigators with the variation of a linear relationship between specific humidity and the corresponding saturation temperature of air adjacent to the fin surface. For determination of the fin surface temperature under this scheme, fin-tip temperature is essentially known a priori which can be employed to calculate the psychrometric parameters associated with the dehumidification process. On the other hand, the tip temperature is only known after the salving the governing equation and it is also a function of the psychrometric properties of air. Thus for the simplicity, dew point temperature is considered as the tip temperature for calculating only the psychrometric parameters of fully wet fins in a recent publication. Nevertheless, in the actual situation this dew point temperature never satisfies at the tip and therefore psychrometric parameters calculated with the assumption of the dew point temperature at the tip may be incorrect. In the present work, an iterative scheme is demonstrated for determination of the actual tip temperature and local fin surface temperature. With considering this aspect, thermal analysis of a new geometric fin, namely, annular step fin (ASF) is proposed for the more effective utilization of fin material in comparison with the annular disc fin. An optimization study has also been made by using the modified thermal analysis of fully wet fins and the analysis of partially wet fins, separately. A remarkable change in results has been noticed when they are compared with that of the published result. Finally, it is worthy to mention that the maximum heat transfer rate per unit volume for an ASF is always higher than that of the annular disc fin for the identical design condition.

1. Introduction

Fin-and-tube heat exchangers are commonly employed to increase the air side heat transfer rate by decrease in thermal resistance. They have wide applications in the field of thermal engineering, especially, in refrigeration and air conditioning equipments in which the physical phenomena such as air cooling and dehumidification are involved, simultaneously. Condensation of humid air on the heat transfer surface takes place when the surface temperature is maintained below the dew point temperature of the surrounding air. The presence of water condensate on the fin surface makes a complicated analysis. The effectiveness of heat exchangers is primarily dependent upon the efficiency of the secondary surface. If the temperature of entire fin surface is higher than the dew point of the surrounding air, there is only sensible heat transferred from the air to the fin so that the fin surface is fully dry. If the temperature of entire fin surface is below the dew point, and both the sensible and latent heat is produced as a result the fin surface becomes fully wet. The fin surface is partially wet if the fin-base temperature is lower than the dew point while the fin-tip temperature is higher than that of the surrounding air.

In most of the applications, the tube geometry of fin-and-tube heat exchangers is circular. In general for the circular tube, circumferential fins are used. It is well known that the annular fin is the better option for transferring heat from the circular primary surface for a constant base temperature. However, the various fin profiles such as constant thickness, louver, convex louver, wavy, etc. are found in the literature of the fin-and-tube heat exchanger's design. Depending upon the applications and design criteria, different shapes of the tube and fins theoretically exist but among of these fin geometries, constant thickness fin is the most popular fin pattern in heat exchanger applications, probably, owing to its simplicity, rigidity and economical impact. The main geometrical components of different types of heat exchangers are made of a circular pipe circumscribing circular fins or continuous plate fins are pierced by the circular pipes.

An intensive research work has already been engaged to determine the fin performance under the simultaneous heat and mass transfer environment. Threlkeld [1] analyzed the effect of condensation on the performance of rectangular fins with the assumption of a uniform condensate film covered on the fin surface. The overall

* Tel.: +91 9433031203; fax: +91 3324146890.
E-mail address: bkundu123@rediffmail.com

0017-9310/$ - see front matter © 2009 Elsevier Ltd. All rights reserved.
doi:10.1016/j.ijheatmasstransfer.2008.12.017

Nomenclature

ASF	annular step fin
A, B	constants evaluated from the fin-base and fin-tip conditions, see Eq. (3b)
Bi	Biot number based on semi-base thickness, ht_0/k
C_p	specific heat of surrounding air (J kg^{-1} K^{-1})
$d's$	dimensionless variables defined in Eq. (13)
D_1, D_2	determinants expressed in Eqs. (24) and (25), respectively
$e's$	dimensionless variables defined in Eq. (14)
f	function defined in Eq. (27)
$f's$	dimensionless variables defined in Eq. (15)
g	function defined in Eq. (28)
$g's$	dimensionless variables used in Eq. (16)
h	convective heat transfer coefficient (W m^{-2} K^{-1})
$h's$	dimensionless variables used in Eq. (17)
h_{fg}	latent heat of condensation of moisture (J kg^{-1})
h_m	mass transfer coefficient (kg m^{-2} S^{-1})
$I_n(Z)$	modified Bessel function of first kind of order n and argument Z
J	Jacobian matrix defined Eq. (30)
k	thermal conductivity of the fin material (W m^{-1} K^{-1})
$K_n(Z)$	modified Bessel function of second kind of order n and argument Z
Le	Lewis number
m, n	defined in Eq. (27)
P	pressure (bar)
q	actual heat transfer rate through the fin (W)
Q	dimensionless actual heat transfer rate, $q/[4\pi k r_i (T_a - T_b)]$
q_i	ideal heat transfer rate through the fin (W)
Q_i	dimensionless ideal heat transfer rate, $q_i/[4\pi k r_i (T_a - T_b)]$
r	radial distance measured from the tube centre (m)
R	dimensionless radial distance, r/r_i
r_i	outer radius of the tube (m)
r_s	radial distance at which step change occurs, see Fig. 1 (m)
R_s	dimensionless radial distance, r_s/r_i
r_0	outer radius of an annular fin, see Fig. 1 (m)
R_0	dimensionless radius, r_0/r_i
RH	relative humidity
t_0	semi-base thickness, see Fig. 1 (m)
t_1	semi-tip thickness, see Fig. 1 (m)
T	temperature (°C)
T_s	fin surface temperature at the section where step change occurs (°C)
U	dimensionless fin volume, defined in Eq. (23)
V	fin volume (m^3)
Z_0	fin parameter, $\sqrt{Bi/\psi}$
Z_1, Z_2, Z_3	dimensionless fin parameters defined in Eq. (5)
Z_4, Z_5, Z_6	dimensionless parameters defined Eq. (9)

Greek symbols

η	fin efficiency
Δ_1, Δ_2	variables defined in Eq. (32)
Γ_1, Γ_2	variables, see Eq. (33)
Ω_1, Ω_2	variables, see Eqs. (34) and (35)
θ	dimensionless temperature, $(T_a - T)/(T_a - T_b)$
θ_p	dimensionless temperature parameter, $(\omega_a - A - BT_a)/[(T_a - T_b)1 + B\xi)]$
θ_s	dimensionless temperature at a radial distant $r = r_s$
ψ	aspect ratio, t_0/r_i
φ	dimensionless temperature parameter, $\theta + \theta_p$
φ_0	dimensionless temperature parameter, $1 + \theta_p$
φ_s	dimensionless temperature parameter at the junction of the step fin $\theta_s + \theta_p$
τ	thickness ratio, t_1/t_0
ω	specific humidity of the surrounding air, kg water vapor/kg dry air
ξ	dimensionless latent heat transfer parameter, $h_{fg}/C_p Le^{2/3}$

Subscripts

a	ambient
b	base
d	dew point
j	jth iteration
opt	optimum
t	tip

fin efficiency has been determined analytically by using the enthalpy difference as the driving force for the combined heat and mass transfer process. He assumed a linear relationship between the air temperature and the corresponding saturated air enthalpy. His model showed that the wet fin efficiency was slightly affected by the air relative humidity. ARI Standard 410-72 [2] used an approach similar to Thelkeld [1], but neglecting the presence of the water film on the surface. McQuiston [3] obtained analytical expressions for the one-dimensional fin efficiency of a rectangular fin, where the calculation of wet fin efficiency is calculated based on a modified dry fin formula. It was shown that the wet fin efficiency is lower than that of a dry fin. The effect of variations of film thickness and local mass transfer has been considered by Coney et al. [4,5] to determine the fully wet fin efficiency of one-dimensional rectangular fin numerically. Their result showed that there is negligible effect of condensate thermal resistance on the fin temperature distribution. Kilic and Onet [6] presented a quasilinearization solution for rectangular fins oriented vertically under a convecting condition when condensation occurs. Their solution was given by assuming that the average heat transfer coefficient is constant along the length of the fin. A summary of the previous studies on condensation over rectangular fins was presented by Srinivasan and Shah [7]. Wu and Bong [8] demonstrated the analysis of partially wet surface of plane rectangular fins. They mentioned that when a fin becomes partially wet the overall efficiency is significantly dependent upon the air relative humidity. Kazeminajad [9] studied a rectangular fin assembly under fully wet condition. To obtain a numerical solution, he used a concept of the sensible to total heat ratio for the psychrometric calculation.

By taking into consideration of the temperature distribution over the fin surface, Elmahdy and Biggs [10] determined the overall fin efficiency of circular wet fins. Their works had been treated separately as heat transfer and mass transfer mechanisms with consideration of respective driving forces. For the analysis of wet fins, they assumed a linear relationship between humidity ratio of the saturated air on the fin surface and the corresponding temperature. The numerical results were indicated that the fin efficiency strongly depends on the relative humidity. Hong and Webb [11] derived an analytical formulation for the fin efficiency of fully wet surfaces for circular fins. For the exact solution of the governing differential equation, they adopted a linear relationship between the humidity ratio and dry bulb temperature. Rosario and Rahman [12] established a one-dimensional radial fin assembly model with condensation. They indicated that the heat transfer

rate enhances with the increment in dry bulb temperature and relative humidity of the air. Naphon [13] presented a theoretical result of the fin efficiency of the annular fin assembly. Sharqawy and Zubair [14] studied analytically the efficiency and optimization of an annular fin with combined heat and mass transfer. They introduced to a new modified fin parameter can be calculated without knowing the actual fin-tip condition. Recently, the analysis of annular fins of constant cross-sectional area with the combined heat and mass transfer mechanisms has been demonstrated by Sharqawy and Zubair [15] numerically.

Wang et al. [16] reported through a systematic study for determining the performance of continuous fin-and-tube heat exchangers under dehumidifying conditions with the variation of design parameters such as inlet conditions, fin spacing and number of tube rows on the heat transfer characteristics. They estimated the fin efficiency by equivalent circular area and sectors methods [17]. A tube-by-tube reduction method for simultaneous heat and mass transfer characteristics for plain fin-and-tube heat exchangers in dehumidifying conditions was proposed by Wang [18]. A different method, namely the finite circular method, was used by Pirompugd et al. [19] to analyze the performance of fin-and-tube heat exchangers having plain fin configuration under fully and partially wet surface conditions. Jang and Lin [20] presented a two-dimensional analysis for the efficiency of continuous plate fin-tube heat exchangers in staggered and inline arrangements under the dry, partially wet and fully wet conditions for different heat transfer coefficient and air relative humidity. The performance of plain and plate-finned circular tube evaporatively cooled heat exchangers was investigated by Hasan and Siren [21] under similar operating conditions of air flow rates and inlet hot temperatures. Alternatively, elliptic cylinder is a typical geometry used in heat exchangers which could take the shape of a flat plate or circular cylinder depending upon the minor and major axis ratio. There may be an advantage when using elliptic tubes as the pumping power needed to flow fluids around the tube is reduced. On the other hand, the elliptic tubes are generally restricted to the low pressure application in the tube side. Lin and Jang [22] presented a two-dimensional analysis for the efficiency of an elliptic fin around of an elliptic tube under the dry, partially wet and fully wet conditions. The effect of dehumidification of air on the performance of eccentric circular fins was carried out numerically by Kazeminajad et al. [23].

It is well known fact that the heat conduction rate from the fin-base to fin-tip gradually decreases for the continuous interaction of energy exchange from the fin surface to the surrounding. Because of that, for the betterment of fin design, fin profile should have a tapered shape. Thus many researchers have already engaged to carryout the analysis of wet fins of taper profiles. Toner et al. [24] determined the fin temperature and the fin effectiveness of the triangular fin with condensation using quasilinearlization techniques and Gauss Seidel iterative method. Kundu [25] studied analytically the effect of dehumidification of air on the performance and optimization of straight taper fins. An analytical method based on the Frobenius power series expansion has been developed by Kundu and Das [26] for prediction of the performance of fully wet fins of different geometries, namely, longitudinal, annular and spine having both the trapezoidal and triangular profiles. They also discussed a method for constructing design curves for the optimum fins. In a recent publication, Kundu [27] has determined the optimum profile of three common types of fins under dehumidifying conditions using calculus of variation.

Although taper fins transfer more rate of heat per unit volume, they are not found in every practical application because of the difficulty in manufacturing and fabrications. On the other hand, constant thickness concentric-annular fins for the circular primary surface are still the common preference. Therefore, there is a scope to modify the geometry of a constant thickness fin in view of the less difficulty in manufacturing and fabrication as well as betterment of heat transfer rate per unit volume of the fin material. For the better utilization of fin material of concentric-annular disc fins, Kundu and Das [28] modified a fin-geometry, namely, annular disc fin with a step change in local thickness. They demonstrated that the heat transfer rate is increased up to 30% by using the modified fin-geometry instead of an annular disc fin for a constant fin volume. However, their analysis was limited for the condition of dry surface fins only. In refrigeration and air conditioning applications, fin surface temperature is normally less than the dew point of the surrounding humid air as a result simultaneous heat and mass transfer occur due to condensation of moisture on the fin surface. The amount of condensation of moisture is mainly dependent upon the humidity ratio of air between the surrounding and that on the fin surface and thus the analysis of wet fin surface differs from that of the dry surface. No research activity has so far been reported in the literature to analyze the performance of step annular disc fins subjected to combined heat and mass transfer conditions.

In the present work, an analytical method is described for temperature and heat transfer characteristics of an ASF with the simultaneous heat and mass transfer mechanisms. Depending upon the psychrometric properties of surrounding air and the fin surface temperature, a fin surface may be fully or partially wet. The present study analyzes an annular fin under fully and partially wet surface conditions. For the calculation of latent heat transfer, specific humidity of saturated air on the fin surface is taken a linear function with the corresponding fin surface temperature. The effects of ambient temperature, ambient pressure, fin-base temperature, relative humidity and thermo-geometric parameters on the fin performances are studied systematically. A methodology has been described for the optimization of circumferential wet fins. To establish the merit of the present analysis of fin performance and optimization, results obtained from both the present and published models have been compared. Unlike previous study, a new procedure for the optimization of fully wet circumferential fins has been addressed. Finally from the optimization study, it can be demonstrated that an ASF is the better choice for transferring rate of heat in comparison with the concentric-annular disc fin for the same fin volume and identical surface conditions.

2. Formulations of the mathematical model

2.1. Performance analysis

The schematic diagram of an ASF with the geometrical details is shown in Fig. 1. This figure depicts a concentric ASF of the base thickness $2t_0$, tip thickness $2t_1(t_0 \geqslant t_1)$ and a circular tube of outer radius r_i. The description of other geometric dimensions of ASFs are a step change of radius r_s and an outer radius r_0. Depending upon the surface temperature of a fin and the dew point temperature of the surrounding air, either sensible or both sensible and latent heat transfer takes place on the fin surface. Therefore, on the basis of heat transfer mechanism, the fin surface can be treated as dry, fully wet or partially wet. To derive the mathematical formulations of the present theoretical model, the thermal conductivity of the fin material and the coefficient of convective heat transfer are assumed to be constant. In this section, it can be mentioned that the dehumidification takes place only on the fin surface when the fin temperature is below the dew point temperature of the surrounding air. The possible wet length of an ASF for a partially wet condition is shown in Fig. 2. For the analysis of fully as well as partially wet surface fins, separate energy equations with respect to their surfaces are necessary. Selecting a cylindrical polar

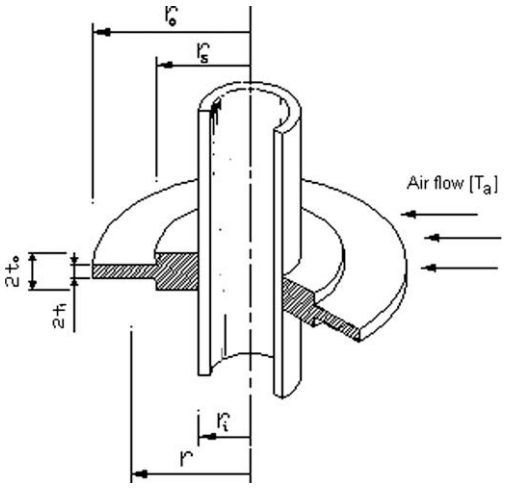

Fig. 1. Schematic diagram of an AFST.

coordinate at the centre of the tube, one-dimensional energy equation for an ASF in wet conditions can be written under steady state as follows:

Fully wet

$$\begin{bmatrix} d(rdT/dr)/dr - hr\{T - T_a + h_m(\omega - \omega_a)h_{fg}/h\}/(kt_0) \\ d(rdT/dr)/dr - hr\{T - T_a + h_m(\omega - \omega_a)h_{fg}/h\}/(kt_1) \end{bmatrix} = \begin{bmatrix} 0 \\ 0 \end{bmatrix} \quad \begin{matrix} \text{for } (r_i \leqslant r \leqslant r_s) \\ \text{for } (r_s \leqslant r \leqslant r_0) \end{matrix} \tag{1a}$$

Partially wet $(r_i < r_d \leqslant r_s)$

$$\begin{bmatrix} d(rdT/dr)/dr - hr\{T - T_a + h_m(\omega - \omega_a)h_{fg}/h\}/(kt_0) \\ d(rdT/dr)/dr - hr(T - T_a)/(kt_0) \\ d(rdT/dr)/dr - hr(T - T_a)/(kt_1) \end{bmatrix} = \begin{bmatrix} 0 \\ 0 \\ 0 \end{bmatrix} \quad \begin{matrix} \text{for } (r_i \leqslant r \leqslant r_d) \\ \text{for } (r_d \leqslant r \leqslant r_s) \\ \text{for } (r_s \leqslant r \leqslant r_0) \end{matrix} \tag{1b}$$

Partially wet $(r_s < r_d < r_0)$

$$\begin{bmatrix} d(rdT/dr)/dr - hr\{T - T_a + h_m(\omega - \omega_a)h_{fg}/h\}/(kt_0) \\ d(rdT/dr)/dr - hr\{T - T_a + h_m(\omega - \omega_a)h_{fg}/h\}/(kt_1) \\ d(rdT/dr)/dr - hr(T - T_a)/(kt_1) \end{bmatrix} = \begin{bmatrix} 0 \\ 0 \\ 0 \end{bmatrix} \quad \begin{matrix} \text{for } (r_i \leqslant r \leqslant r_s) \\ \text{for } (r_s \leqslant r \leqslant r_d) \\ \text{for } (r_d \leqslant r \leqslant r_0) \end{matrix} \tag{1c}$$

The heat and mass transfer coefficients can be related by the Chilton–Colburn analogy [29]:

$$h/h_m = c_p Le^{2/3} \tag{2}$$

Equation (1) cannot be solved because of the two dependent variables T and ω. Due to formation of small thickness of condensate on the fin surface, the condensate resistance is negligibly small as a result there is no temperature gradient in the transverse direction of the condensate. Thus, the local condensate temperature is equal to the corresponding fin surface temperature. The condensate is surrounded by a saturated humid air with the same condensate temperature. Therefore, T and ω can be related with the psychrometric relations. In order to obtain an analytical solution, many investigators [3,8,14,25–27,30] have assumed the above relationship to be a linear one and they have also justified for the assumption of the linear relationship. In the present work, a linear model is used to calculate the mass driving force.

$$\omega = A + BT \tag{3a}$$

A and B in Eq. (3) are constants determined by Wu and Bong [8] from the condition of fin-base and fin-tip.

$$\begin{bmatrix} A \\ B \end{bmatrix} = \begin{bmatrix} \{(T_t - T_b)\omega_t - (\omega_t - \omega_b)T_t\}/(T_t - T_b) \\ (\omega_t - \omega_b)/(T_t - T_b) \end{bmatrix} \tag{3b}$$

From Eq. (3), it is clear that A and B are dependent upon the tip and base temperature. For the analysis of individual fins, base temperature is a known design constant. The temperature distribution in the fin is determined by solving the energy equation using the base temperature along with the tip boundary condition. Thus the closed form expressions of A and B are not possible because these are as a function of unknown tip temperature to be determined from the solution of the governing equation. To avoid

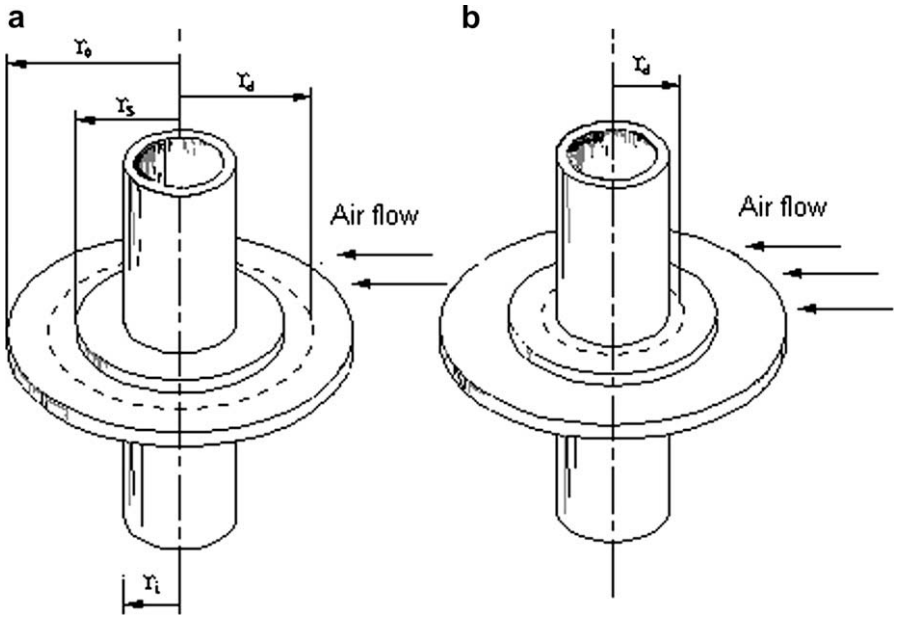

Fig. 2. Radial distance of wet length R_d for the partially wet surface fin: (a) $r_s \leqslant r_d < r_0$ and (b) $r_i < r_d \leqslant r_s$.

the above complexity, Sharqawy and Zubair [14] have suggested a scheme for calculation of psychrometric properties at the tip with the help of the dew point temperature instead of the tip temperature. The dew point temperature is a design known parameter which can be determined directly from the psychrometric properties of surrounding air. In this regard, it is worthy to mention that in actual situation, the tip temperature for the fully wet fin may not be equal to the dew point temperature. Thus for the calculation of A and B with consideration of the dew point temperature at the tip, it is not an appropriate procedure. In the present paper A and B as well as tip temperature for a fully wet fin are determined through iteration. Initially tip temperature is assumed to be a dew point temperature and then A and B are calculated. With these known variables, tip temperature is estimated by solving governing differential equation. If the difference between initial and calculated tip temperatures differs and then A and B are determined with the present calculated tip temperature and the procedure can be repeated until the present and previous values are the same or difference of these is very small (10^{-6}).

Substituting Eqs. (2) and (3) in Eq. (1), the following expressions can be written in normalized form as

Fully wet

$$\begin{bmatrix} d(Rd\phi/dR)/dR - Z_1^2 R\phi \\ d(Rd\phi/dR)/dR - Z_2^2 R\phi \end{bmatrix} = \begin{bmatrix} 0 \\ 0 \end{bmatrix} \quad \begin{matrix} \text{for } (1 \leqslant R \leqslant R_s) \\ \text{for } (R_s \leqslant R \leqslant R_0) \end{matrix} \tag{4a}$$

Partially wet ($1 < R_d \leqslant R_s$)

$$\begin{bmatrix} d(Rd\phi/dR)/dR - Z_1^2 R\phi \\ d(Rd\theta/dR)/dR - Z_0^2 R\theta \\ d(Rd\theta/dR)/dR - Z_3^2 R\theta \end{bmatrix} = \begin{bmatrix} 0 \\ 0 \\ 0 \end{bmatrix} \quad \begin{matrix} \text{for } (1 \leqslant R \leqslant R_d) \\ \text{for } (R_d \leqslant R \leqslant R_s) \\ \text{for } (R_s \leqslant R \leqslant R_0) \end{matrix} \tag{4b}$$

Partially wet ($R_s < R_d < R_0$)

$$\begin{bmatrix} d(Rd\phi/dR)/dR - Z_1^2 R\phi \\ d(Rd\phi/dR)/dR - Z_2^2 R\phi \\ d(Rd\theta/dR)/dR - Z_3^2 R\theta \end{bmatrix} = \begin{bmatrix} 0 \\ 0 \\ 0 \end{bmatrix} \quad \begin{matrix} \text{for } (1 \leqslant R \leqslant R_s) \\ \text{for } (R_s \leqslant R \leqslant R_d) \\ \text{for } (R_d \leqslant R \leqslant R_0) \end{matrix} \tag{4c}$$

where

$$\begin{aligned} &R = r/r_i,\ R_s = r_s/r_i,\ R_d = r_d/r_i,\ R_0 = r_0/r_i,\ Bi = hr_i/k, \\ &\psi = t_0/r_i,\ \tau = t_1/t_0, \\ &\theta = (T_a - T)/(T_a - T_b),\ Z_0 = \sqrt{Bi/\psi},\ Z_1 = Z_0(1 + B\xi)^{1/2}, \\ &Z_2 = Z_3(1 + B\xi)^{1/2},\ Z_3 = Z_0/\sqrt{\tau}, \\ &\theta_p = (\omega_a - A - BT_a)/\{(T_a - T_b)(1 + B\xi)\} \quad \text{and} \quad \phi = \theta + \theta_p \end{aligned} \tag{5}$$

Equation (4) can be solved by using appropriate boundary conditions. For the solution of fully wet surface, four boundary conditions, namely, a constant fin-base temperature, an energy balance and continuity of temperature at the section where a step change in thickness occurs, and the energy interaction through the tip with the surrounding are considered. In the case of partially wet fins, an additional condition at the section at which the wet part separates from the dry part is required. Thus to solve Eq. (4), the boundary conditions are taken mathematically as follows:

Boundary conditions for the fully wet

$$\text{at} \quad R = 1, \phi = \phi_0 \tag{6a}$$

$$\text{at} \quad R = R_s, \begin{cases} \phi = \phi_s \\ (d\phi/dR)_{R_s - \delta} = \tau(d\phi/dR)_{R_s + \delta} - Z_4\phi_s \end{cases} \tag{6b}$$

$$\text{at} \quad R = R_0,\ d\phi/dR = -Z_5\phi \tag{6c}$$

Boundary conditions for the partially wet fin ($1 < R_d \leqslant R_s$)

$$\text{at} \quad R = 1,\ \phi = \phi_0 \tag{7a}$$

$$\text{at} \quad R = R_d, \begin{cases} \phi = \phi_d \\ (d\phi/dR)_{R_d - \delta} = (d\theta/dR)_{R_d + \delta} \end{cases} \tag{7b}$$

$$\text{at} \quad R = R_s, \begin{cases} \theta = \theta_s \\ (d\theta/dR)_{R_s - \delta} = \tau(d\theta/dR)_{R_s + \delta} - Z_6\theta_s \end{cases} \tag{7c}$$

$$\text{at} \quad R = R_0,\ d\theta/dR = -Bi\theta \tag{7d}$$

Boundary conditions for the partially wet fin ($R_s < R_d \leqslant R_0$)

$$\text{at} \quad R = 1,\ \phi = \phi_0 \tag{8a}$$

$$\text{at} \quad R = R_s, \begin{cases} \phi = \phi_s \\ (d\phi/dR)_{R_s - \delta} = \tau(d\phi/dR)_{R_s + \delta} - Z_4\phi_s \end{cases} \tag{8b}$$

$$\text{at} \quad R = R_d, \begin{cases} \phi = \phi_d \\ (d\phi/dR)_{R_d - \delta} = (d\theta/dR)_{R_d + \delta} \end{cases} \tag{8c}$$

$$\text{at} \quad R = R_0,\ d\theta/dR = -Bi\theta \tag{8d}$$

where

$$Z_4 = Bi(1 - \tau)(1 + B\xi), \quad Z_5 = Bi(1 + B\xi), \quad Z_6 = Bi(1 - \tau), \quad \phi_0 = 1 + \theta_p \quad \text{and} \quad \delta \to 0 \tag{9}$$

The temperature distribution in a fin for both the fully and partially wet surface is determined by solving Eq. (4) along with the boundary conditions (Eqs. (6)–(8)) and it can be expressed for different surfaces as follows:

$$\phi = \frac{\phi_0[I_0(Z_1R)K_0(Z_1R_s) - I_0(Z_1R_s)K_0(Z_1R)] + \phi_s[I_0(Z_1)K_0(Z_1R) - I_0(Z_1R)K_0(Z_1)]}{I_0(Z_1)K_0(Z_1R_s) - I_0(Z_1R_s)K_0(Z_1)} \quad \text{for } (1 \leqslant R \leqslant R_s) \tag{10a}$$

$$\frac{\phi}{\phi_s} = \frac{Z_5[I_0(Z_2R)K_0(Z_2R_0) - I_0(Z_2R_0)K_0(Z_2R)] - Z_2[I_0(Z_2R)K_1(Z_2R_0) + I_1(Z_2R_0)K_0(Z_2R)]}{Z_5[I_0(Z_2R_s)K_0(Z_2R_0) - I_0(Z_2R_0)K_0(Z_2R_s)] - Z_2[I_0(Z_2R_s)K_1(Z_2R_0) + I_1(Z_2R_0)K_0(Z_2R_s)]} \quad \text{for } (R_s \leqslant R \leqslant R_0) \tag{10b}$$

Partially wet surface ($1 < R_d \leqslant R_s$)

$$\phi = \frac{\phi_0[I_0(Z_1R)K_0(Z_1R_d) - I_0(Z_1R_d)K_0(Z_1R)] + \phi_d[I_0(Z_1)K_0(Z_1R) - I_0(Z_1R)K_0(Z_1)]}{I_0(Z_1)K_0(Z_1R_d) - I_0(Z_1R_d)K_0(Z_1)} \quad \text{for } (1 \leqslant R \leqslant R_d) \tag{11a}$$

$$\theta = \frac{\theta_d[I_0(Z_0R)K_0(Z_0R_s) - I_0(Z_0R_s)K_0(Z_0R)] + \theta_s[I_0(Z_0R_d)K_0(Z_0R) - I_0(Z_0R)K_0(Z_0R_d)]}{I_0(Z_0R_d)K_0(Z_0R_s) - I_0(Z_0R_s)K_0(Z_0R_d)} \quad \text{for } (R_d \leqslant R \leqslant R_s) \tag{11b}$$

$$\frac{\theta}{\theta_s} = \frac{Bi[I_0(Z_3R)K_0(Z_3R_0) - I_0(Z_3R_0)K_0(Z_3R)] - Z_3[I_0(Z_3R)K_1(Z_3R_0) + I_1(Z_3R_0)K_0(Z_3R)]}{Bi[I_0(Z_3R_s)K_0(Z_3R_0) - I_0(Z_3R_0)K_0(Z_3R_s)] - Z_3[I_0(Z_3R_s)K_1(Z_3R_0) + I_1(Z_3R_0)K_0(Z_3R_s)]} \quad \text{for } (R_s \leqslant R \leqslant R_0) \tag{11c}$$

Partially wet surface ($R_s < R_d < R_0$)

$$\phi = \frac{\phi_0[I_0(Z_1R)K_0(Z_1R_s) - I_0(Z_1R_s)K_0(Z_1R)] + \phi_s[I_0(Z_1)K_0(Z_1R) - I_0(Z_1R)K_0(Z_1)]}{I_0(Z_1)K_0(Z_1R_s) - I_0(Z_1R_s)K_0(Z_1)} \quad \text{for } (1 \leqslant R \leqslant R_s) \tag{12a}$$

$$\phi = \frac{\phi_s[I_0(Z_2R)K_0(Z_2R_d) - I_0(Z_2R_d)K_0(Z_2R)] + \phi_d[I_0(Z_2R_s)K_0(Z_2R) - I_0(Z_2R)K_0(Z_2R_s)]}{I_0(Z_2R_s)K_0(Z_2R_d) - I_0(Z_2R_d)K_0(Z_2R_s)} \quad \text{for } (R_s \leqslant R \leqslant R_d) \tag{12b}$$

$$\frac{\theta}{\theta_d} = \frac{Bi[I_0(Z_3R)K_0(Z_3R_0) - I_0(Z_3R_0)K_0(Z_3R)] - Z_3[I_0(Z_3R)K_1(Z_3R_0) + I_1(Z_3R_0)K_0(Z_3R)]}{Bi[I_0(Z_3R_d)K_0(Z_3R_0) - I_0(Z_3R_0)K_0(Z_3R_d)] - Z_3[I_0(Z_3R_d)K_1(Z_3R_0) + I_1(Z_3R_0)K_0(Z_3R_d)]} \quad \text{for } (R_d \leqslant R \leqslant R_0) \tag{12c}$$

Fully wet surface

Eqs. (10)–(12) indicate the temperature distributions in an ASF under the fully wet and partially wet surface conditions. However, in order to determine the temperature in the fin, it may be noted that the unknown temperature θ_s is required and this unknown can be calculated by satisfying an energy balance at the section where fin thickness varies.

Fully wet surface

$$\phi_s = \phi_0 d_1 Z_1 (d_2 Z_5 - d_3 Z_2)/[\tau d_4 Z_2 (d_5 Z_5 - d_6 Z_2) + (d_2 Z_5 - d_3 Z_2)(d_7 Z_1 - d_4 Z_4)] \tag{13a}$$

where

$$d_1 = I_1(Z_1R_s)K_0(Z_1R_s) + I_0(Z_1R_s)K_1(Z_1R_s) \tag{13b}$$
$$d_2 = I_0(Z_2R_s)K_0(Z_2R_0) - I_0(Z_2R_0)K_0(Z_2R_s) \tag{13c}$$
$$d_3 = I_0(Z_2R_s)K_1(Z_2R_0) + I_1(Z_2R_0)K_0(Z_2R_s) \tag{13d}$$
$$d_4 = I_0(Z_1)K_0(Z_1R_s) - I_0(Z_1R_s)K_0(Z_1) \tag{13e}$$
$$d_5 = I_1(Z_2R_s)K_0(Z_2R_0) + I_0(Z_2R_0)K_1(Z_2R_s) \tag{13f}$$
$$d_6 = I_1(Z_2R_s)K_1(Z_2R_0) - I_1(Z_2R_0)K_1(Z_2R_s) \tag{13g}$$

and

$$d_7 = I_0(Z_1)K_1(Z_1R_s) + I_1(Z_1R_s)K_0(Z_1) \tag{13h}$$

Partially wet surface $(1 < R_d \leqslant R_s)$

$$\phi_s = \theta_d Z_0 e_1/[Z_0 e_5 - Z_6 e_3 - \tau Z_3 e_3 (Z_3 e_4 - Bie_6)/(Bie_7 - Z_3 e_2)] \tag{14a}$$

where

$$e_1 = I_1(Z_0R_s)K_0(Z_0R_s) + I_0(Z_0R_s)K_1(Z_0R_s) \tag{14b}$$
$$e_2 = I_0(Z_3R_s)K_1(Z_3R_0) + I_1(Z_3R_0)K_0(Z_3R_s) \tag{14c}$$
$$e_3 = I_0(Z_0R_d)K_0(Z_0R_s) - I_0(Z_0R_s)K_0(Z_0R_d) \tag{14d}$$
$$e_4 = I_1(Z_3R_s)K_1(Z_3R_0) - I_1(Z_3R_0)K_1(Z_3R_s) \tag{14e}$$
$$e_5 = I_0(Z_0R_d)K_1(Z_0R_s) + I_1(Z_0R_s)K_0(Z_0R_d) \tag{14f}$$
$$e_6 = I_1(Z_3R_s)K_0(Z_3R_0) + I_0(Z_3R_0)K_1(Z_3R_s) \tag{14g}$$

and

$$e_7 = I_0(Z_3R_s)K_0(Z_3R_0) + I_0(Z_3R_0)K_0(Z_3R_s) \tag{14h}$$

Partially wet surface $(R_s < R_d < R_0)$

$$\phi_s = (\phi_0 f_1 f_2 Z_1 + \tau\phi_d f_3 f_4 Z_2)/(f_2 f_5 Z_1 + \tau f_3 f_6 Z_2 - f_2 f_3 Z_4) \tag{15a}$$

where

$$f_1 = I_1(Z_1R_s)K_0(Z_1R_s) + I_0(Z_1R_s)K_1(Z_1R_s) \tag{15b}$$
$$f_2 = I_0(Z_2R_s)K_0(Z_2R_d) - I_0(Z_2R_d)K_0(Z_2R_s) \tag{15c}$$
$$f_3 = I_0(Z_1)K_0(Z_1R_s) - I_0(Z_1R_s)K_0(Z_1) \tag{15d}$$
$$f_4 = I_0(Z_2R_s)K_1(Z_2R_s) + I_1(Z_2R_s)K_0(Z_2R_s) \tag{15e}$$
$$f_5 = I_0(Z_1)K_1(Z_1R_s) + I_1(Z_1R_s)K_0(Z_1) \tag{15f}$$

and

$$f_6 = I_1(Z_2R_s)K_0(Z_2R_d) + I_0(Z_2R_d)K_1(Z_2R_s) \tag{15g}$$

In the case of partially wet fin, temperature in a fin at the section where thickness changes is also dependent upon the wet length R_d. Therefore for knowing the temperature distribution, the calculation of radial length R_d is essential. It can be computed by applying the continuity of heat conduction rate at the section where dry and wet parts coexist.

Partially wet surface $(1 < R_d \leqslant R_s)$

$$G(R_d) = [Z_1 g_1(\phi_0 g_2 - \phi_d g_3) - g_4 Z_0(\theta_d g_5 - \theta_s g_6)]/(g_1 g_4) = 0 \tag{16a}$$

where

$$g_1 = I_0(Z_0R_d)K_0(Z_0R_s) - I_0(Z_0R_s)K_0(Z_0R_d) \tag{16b}$$
$$g_2 = I_1(Z_1R_d)K_0(Z_1R_d) + I_0(Z_1R_d)K_1(Z_1R_d) \tag{16c}$$
$$g_3 = I_0(Z_1)K_1(Z_1R_d) + I_1(Z_1R_d)K_0(Z_1) \tag{16d}$$
$$g_4 = I_0(Z_1)K_0(Z_1R_d) - I_0(Z_1R_d)K_0(Z_1) \tag{16e}$$
$$g_5 = I_1(Z_0R_d)K_0(Z_0R_s) + I_0(Z_0R_s)K_1(Z_0R_d) \tag{16f}$$

and

$$g_6 = I_0(Z_0R_d)K_1(Z_0R_d) + I_1(Z_0R_d)K_0(Z_0R_d) \tag{16g}$$

Partially wet surface $(R_s < R_d < R_0)$

$$G(R_d) = Z_2(\phi_s h_1 - \phi_d h_2)/h_3 - \theta_d Z_3(Bi\, h_4 - Z_3 h_5)/(Bi\, h_6 - Z_3 h_7) = 0 \tag{17a}$$

where

$$h_1 = I_1(Z_2R_d)K_0(Z_2R_d) + I_0(Z_2R_d)K_1(Z_2R_d) \tag{17b}$$
$$h_2 = I_0(Z_2R_s)K_1(Z_2R_d) + I_1(Z_2R_d)K_0(Z_2R_s) \tag{17c}$$
$$h_3 = I_0(Z_2R_s)K_0(Z_2R_d) - I_0(Z_2R_d)K_0(Z_2R_s) \tag{17d}$$
$$h_4 = I_1(Z_3R_d)K_0(Z_3R_0) + I_0(Z_3R_0)K_1(Z_3R_d) \tag{17e}$$
$$h_5 = I_1(Z_3R_d)K_1(Z_3R_0) - I_1(Z_2R_0)K_1(Z_3R_d) \tag{17f}$$
$$h_6 = I_0(Z_3R_d)K_0(Z_3R_0) - I_0(Z_3R_0)K_0(Z_3R_d) \tag{17g}$$

and

$$h_7 = I_0(Z_3R_d)K_1(Z_3R_0) + I_1(Z_3R_0)K_0(Z_3R_d) \tag{17h}$$

From Eqs. (16) and (17), it is obvious that the linear distance R_d is a function of thermo-geometric and psychrometric parameters. For a given design condition, R_d can be calculated by solving Eqs. (16) and (17) using Newton–Raphson iterative method [31]. For the numerical iterations, final values of R_d are obtained after satisfying a convergence criterion (10^{-6}).

After obtaining temperature distribution in a fin, actual heat transfer rate through the fin has been estimated by applying the Fourier's law of heat conduction at the fin-base. The actual heat transfer rate can be expressed in dimensionless form as

Fully wet surface

$$Q = \frac{\phi_s[I_0(Z_1)K_1(Z_1) + I_1(Z_1)K_0(Z_1)] - \phi_0[I_1(Z_1)K_0(Z_1R_s) + I_0(Z_1R_s)K_1(Z_1)]}{[I_0(Z_1)K_0(Z_1R_s) - I_0(Z_1R_s)K_0(Z_1)](\psi Z_1)^{-1}} \tag{18a}$$

Partially wet surface $(1 < R_d \leqslant R_s)$

$$Q = \frac{\phi_d[I_0(Z_1)K_1(Z_1) + I_1(Z_1)K_0(Z_1) - \phi_0[I_1(Z_1)K_0(Z_1R_d) + I_0(Z_1R_d)K_1(Z_1)]}{[I_0(Z_1)K_0(Z_1R_d) - I_0(Z_1R_d)K_0(Z_1)](\psi Z_1)^{-1}} \tag{18b}$$

Partially wet surface ($R_s < R_d < R_0$)

$$Q = \frac{\phi_s[I_0(Z_1)K_1(Z_1)+I_1(Z_1)K_0(Z_1)] - \phi_0[I_1(Z_1)K_0(Z_1R_s)+I_0(Z_1R_s)K_1(Z_1)]}{[I_0(Z_1)K_0(Z_1R_s)-I_0(Z_1R_s)K_0(Z_1)](\psi Z_1)^{-1}} \tag{18c}$$

Fin efficiency is commonly used as a fin performance indicator. The fin efficiency is defined as the ratio of the actual heat rate through a fin to the rate of heat that would be transferred ideally if the entire fin surface were maintained at its base temperature. For both the fully and partially wet surfaces, the ideal heat transfer rate is calculated on the basis of fully wet conditions and it can be written in nondimensionalized form as

$$Q_i = (1+B\xi)(1+\theta_p)Bi[(R_0^2-1)/2 + \psi\{R_s(1-\tau)+R_0\}] \tag{19}$$

From definition of the fin efficiency,

$$\eta = Q/Q_i \tag{20}$$

2.2. Optimization analysis

The optimization study of any fin can be done either by maximizing the rate of heat transfer for a given fin volume or by minimizing fin volume for a given heat transfer rate but the result obtained from both the optimization schemes yield the same value. However, selection of the objective function and constraint equations depends upon the requirement of a design. In the present study, an optimization model is proposed in a generalized way with satisfying the above fact. The volume V of an ASF can be expressed in dimensionless form as

$$U = V/2\pi r_i^3 = \psi[R_s^2 - 1 + \tau(R_0^2 - R_s^2)] \tag{21}$$

From Eqs. (18) and (21), it can be transparent that the heat transfer rate and fin volume are of a function of the geometrical parameters ψ, τ, R_s and R_0, and the thermo-physical and psychrometric properties of air. In the previous all optimization studies, the procedure for determination of the design parameters such as θ_p, B and ξ are treated as an explicit function. However, in the actual case of dehumidification of air on the fully wet fin surface, these parameters θ_p, B and ξ are functions of psychrometric conditions as well as fin-tip and fin-base temperatures. For the partially wet fin, they are sole function of the psychrometric condition of air and fin-base temperature. Nevertheless, for the fully wet fin, tip temperature is also dependent upon the above geometrical parameters and Bi. Therefore, unlike the partially wet fin, the aforementioned parameters for the fully wet surface are implicitly connected with the optimization process. In this section, it is noteworthy to mention once again that for the optimization of wet fins, previous researchers have not mentioned a dependency function of the parameters θ_p, B and ξ on the geometrical variables. Recently, Sharqawy and Zubair [14] have considered the tip temperature equal to the dew point temperature for estimating psychrometric parameters for the fully wet fin. However, this consideration may not be always satisfied in actual applications. Therefore, optimization analysis presented by Sharqawy and Zubair [14] may not be a better approximation method. In the present study, a methodology has been proposed for the optimization with considering the above actual fact. In the case of partially wet surface fins, heat transfer rate depends not only on these four geometrical variables but also on the R_d and this dimensionless radius R_d is also function of other variables. Therefore in partially wet condition, the number of dependence variables in the optimization process is the same as the fully wet fin. Thus the optimization of an ASF constitutes a four variable one constraint problem treating either the fin volume or heat transfer rate as a constraint condition. From the manufacturing point of view, the geometrical parameters R_s and τ can be considered as a constraint. Thus the present optimization analysis has been done with varying two variables and a given thermo-psychrometric parameters. Following the methodology of Stoecker [32], the condition of optimality can be derived using the Lagrange multiplier technique. Elimination of the multiplier from the Euler equations gives the following optimality expression:

$$(\partial Q/\partial R_0)(\partial U/\partial \psi) - (\partial Q/\partial \psi)(\partial U/\partial R_0) = 0 \tag{22}$$

In order to expand Eq. (22), the mathematical expressions of Q and U are required which are as a function of ψ and R_0. It may be noted that there are three equations used for the expression of Q. For the analysis of the fin optimization, it is thus required a unified expression of Q instead of three and it can be written as

$$Q = \psi Z_1 D_1/D_2 \tag{23}$$

where

$$D_1 = \begin{vmatrix} m & 0 & \phi_0 \\ I_0(Z_1 n) & I_1(Z_1) & I_0(Z_1) \\ K_0(Z_1 n) & -K_1(Z_1) & K_0(Z_1) \end{vmatrix} \tag{24}$$

$$D_2 = \begin{vmatrix} I_0(Z_1) & I_0(Z_1 n) \\ K_0(Z_1) & K_0(Z_1 n) \end{vmatrix} \tag{25}$$

and

$$(m,n) = \begin{cases} (\phi_s, R_s) & \text{for fully wet and partailly wet } (R_s \leqslant R_d \leqslant R_0) \\ (\phi_d, R_d) & \text{for partailly wet } (1 \leqslant R_d \leqslant R_s) \end{cases} \tag{26}$$

Eq. (22) is now expanded by using Eqs. (21) and (23) as

$$\begin{aligned} f(R_0,\psi) = {} & (D_2\partial D_1/\partial R_0 - D_1\partial D_2/\partial R_0)[R_s^2 - 1 + \tau(R_0^2 - R_s^2)] \\ & - \tau R_0[2D_1D_2 + 2\psi(D_2\partial D_1/\partial\psi - D_1\partial D_2/\partial\psi)] = 0 \end{aligned} \tag{27}$$

In order to determine the optimum parameters, Eq. (27) can be solved along with the constraint either heat transfer rate (Eq. (23)) or fin volume (Eq. (21)) depending upon the requirement of a design. Thus the constraint equation can be formed by combining Eqs. (21) and (23) as follows:

$$g(R_0,\psi) = 0 = \begin{cases} \psi Z_1 D_1/D_2 - Q \\ \psi[R_s^2 - 1 + \tau(R_0^2 - R_s^2)] - U \end{cases} \tag{28}$$

A numerical scheme, namely Newton–Raphson iterative method [28], is adopted for solving Eqs. (27) and (28). For finding the multiple roots by Newton–Raphson method, it is worthy to mention that the initial guess values for the roots have been taken cautiously so that the convergence criteria for each iteration has been satisfied [28]. For the present problem, a brief outline of the generalized Newton–Raphson method and the convergence criteria for each step of iterations are described in the following paragraph.The optimum values of design variables such as R_0 and ψ can be approximated from the Newton–Raphson formula by using justly previous iterative or initial guess values of these variables.

$$\begin{bmatrix} R_{0j+1} \\ \psi_{j+1} \end{bmatrix} = \begin{bmatrix} R_{0_j} \\ \psi_j \end{bmatrix} - [J(R_{0j},\psi_j)]^{-1} \begin{bmatrix} f(R_{0j},\psi_j) \\ g(R_{0j},\psi_j) \end{bmatrix} \tag{29}$$

where J denotes the Jacobian matrix which can be expressed as

$$[J(R_{0j},\psi_j)] = \begin{bmatrix} (\partial f/\partial R_0)_j & (\partial f/\partial\psi)_j \\ (\partial g/\partial R_0)_j & (\partial g/\partial\psi)_j \end{bmatrix} \tag{30}$$

The subscript "j" denotes the value of jth iteration. The convergence criteria given below at each step of iteration must be satisfied.

$$\text{Max}\{\Delta_1, \Delta_2\} < 1 \tag{31}$$

where the expressions for Δ_1 and Δ_2 are given by

$$\begin{bmatrix} \Delta_1 \\ \Delta_2 \end{bmatrix} = \begin{bmatrix} |\partial\Gamma_1/\partial \mathrm{R}_0|_j + |\partial\Gamma_2/\partial \mathrm{R}_0|_j \\ |\partial\Gamma_1/\partial\psi|_j + |\partial\Gamma_2/\partial\psi|_j \end{bmatrix} \tag{32}$$

$$\begin{bmatrix} \Gamma_1 \\ \Gamma_2 \end{bmatrix} = \begin{bmatrix} \mathrm{R}_0 - \mathrm{Det}\Omega_1/\mathrm{Det}J \\ \psi - \mathrm{Det}\Omega_2/\mathrm{Det}J \end{bmatrix} \tag{33}$$

$$[\Omega_1] = \begin{bmatrix} f & \partial f/\partial\psi \\ g & \partial g/\partial\psi \end{bmatrix} \tag{34}$$

and

$$[\Omega_2] = \begin{bmatrix} \partial f/\partial \mathrm{R}_0 & f \\ \partial g/\partial \mathrm{R}_0 & g \end{bmatrix} \tag{35}$$

The above procedures are repeated till the geometrical roots R_0 and ψ are obtained to a desired accuracy (10^{-6} in the present study).

3. Results and discussion

Based on the above analysis, results have been generated for a wide range of thermo-psychrometric parameters. Due to presence of concentration gradient of moisture-vapor between the ambient and fin surface, condensation of moisture on the fin surface takes place. During condensation, latent heat is released. The partial pressure of water vapor in the air depends on the relative humidity of air and the saturation vapor pressure corresponding to the ambient temperature. The water vapor is condensed at a constant partial pressure. The condensation process also follows a constant temperature which is equal to the dew point temperature. During the condensation, an equilibrium condensate temperature is attained which may be equal to the fin surface temperature because of the formation of negligible condensate thickness. As the fin surface temperature gradually decreases from the fin-tip to fin-base, thus the condensate temperature in the radial direction on the fin surface changes. The humid air adjacent to the condensate becomes saturated with the corresponding condensate temperature. Therefore, temperature of the saturated air adjoining to the fin surface varies along the fin length. The humidity ratio of air on the fin surface can be calculated by using saturation temperature and thus it becomes a sole function of their temperatures.

In order to make a comparison between the present and published works, Fig. 3 is depicted. For the analysis of annular disc fins, the present analysis of ASF is equally suitable for the consideration of the geometrical parameter $\tau = 1$. From the previous study [14], temperature distribution on the fin surface is obtained with considering the tip temperature equal to the dew point temperature for calculating psychrometric properties of air. However, it is interesting to mention that for determination of temperature profile, insulated tip condition is also taken. Thus two conditions at the tip and one at the base were used for their calculations. In actual case, tip temperature may not be equal to the dew point temperature of the surrounding air and thus in the present study, an iteration scheme is established to determine the actual temperature distribution in the fin. The result obtained from the method followed by Wu and Bong [8] for an annular disc fin is plotted in the same figure. In the Wu and Bong [8] paper, there was no instruction given for calculating the tip temperature and latent heat of condensation. Moreover, both the results obtained from the present study and Wu and Bong methodology [8] are matched exactly whereas Sharqawy and Zubair [14] predicted a difference in results and the magnitude of difference gradually increases with the increase in both relative humidity and length. From the figure, it can also be mentioned that for the range of psycho-geometric parameters taken, a fully wet condition is maintained on the fin surface. For comparison between dry and wet surface, temperature for the dry surface is also illustrated. From the temperature distribution for wet surface fins, it can be highlighted that with the consideration of dew point temperature at the tip, fin surface temperature is always an over predict in comparison to the actual surface temperature.

For the validation of the present model, a numerical scheme followed by finite difference method is used. Difference equations are derived by discretization of governing equations of the present paper using the Taylor series central difference scheme for second order of accuracy. These difference equations are simultaneously solved at the pivotal points by Gauss Seidel iterative method with satisfying their appropriate boundary conditions and convergence criterion (10^{-6}). In order to make grid independency on the computational solution for the domain, it is done with the consideration of 75, 100 and 125 grid points. Taking results with the adaptation of aforementioned grid points, it may be pointed that a slight variation of results (<0.1%) has been obtained when results are taken for the selection of 100 grid points instead of 75. On the other hand, no significant variation has been noticed between the results obtained for 100 and 125 grid points. Thus the present numerical result has been determined with the selection of 100 nodal points. Fig. 4 depicts a comparison of temperature distribution in an ASF predicted by present analytical and numerical methods.

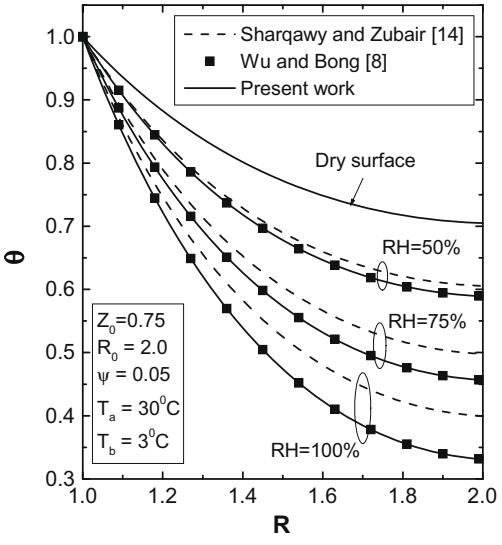

Fig. 3. Variation of dimensionless temperature with the radial distance for an annular disc fin under both the dry and wet surface conditions.

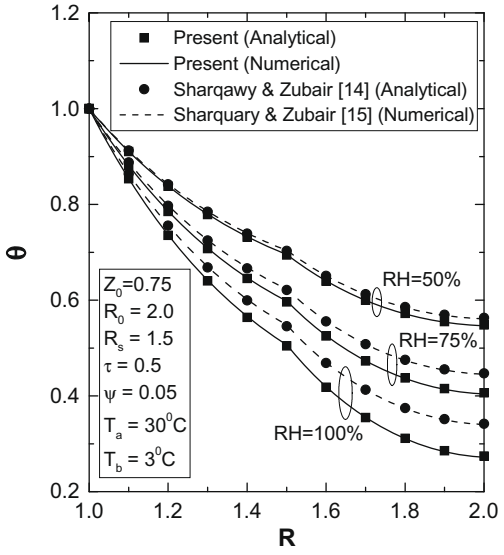

Fig. 4. Validation of the present results with the numerical values.

For comparison of Sharqawy and Zubair analyses (i.e. calculation of psychrometric properties of air at the tip based on the dew point temperature), the analytical [14] and the corresponding numerical values [15] are exhibited in the same figure, and it is shown that both analytical and numerical predictions are matched convincingly with a high accuracy.

Now temperature distribution for ASFs for the dry and wet surface conditions is depicted in Fig. 5 for the geometrical parameters $\tau = 0.5$ and $R_s = 1.5$, and in comparison, results obtained from existing methods of analysis are also plotted in the same figure. Again an erroneous temperature prediction is noticed while considering tip temperature as a dew point temperature. Temperature distribution for the ASF always differs from that for the annular disc fin which can be clearly understandable by comparing Figs. 3 and 5. Like previous study with the increase in relative humidity, absolute fin temperature increases due to increase in rate of condensation as a result of more evolving latent heat of condensation. Once again, results obtained from the present and Wu and Bong methodology [8] gives the same value. Tip temperature for ASFs under fully wet surface conditions is always higher than that for the annular disc fin due to increase in conductive resistance near the tip of ASFs. Again from the temperature distribution of a step fin, it can be demonstrated that the variation of temperature along the radial direction changes at different rate in the respective base and tip thickness sections as shown in Fig. 5.

A surface becoming fully wet, partially wet or dry is mainly dependent upon the relative humidity and thermo-geometric parameters. For the analysis of partially wet surface fin, it is always necessary to calculate the radial distance R_d at which dry and wet surface separates. The variation of R_d as a function of relative humidity for ASFs is depicted in Fig. 6 for different τ values. The range of relative humidity for maintaining a partially wet surface is shown a minimum value for annular disc fins and is comparatively larger for ASFs, however, it is also function of the geometrical parameter τ. From Fig. 6, it can be mentioned that due to small range of relative humidity noticed, a partially wet surface may not be found in actual design conditions and thus there is a high possibility to satisfy a fully wet surface condition. Therefore, an extra attention may be given in the design of wet fin with consideration of the fully wet conditions. The same result is also found for the method followed by Wu and Bong [8].

After getting the temperature distribution, fin efficiency for annular disc fins under wet conditions is determined from the present analysis of ASFs with the consideration of equal thickness ratio which is depicted in Fig. 7 as a function of the fin parameter Z_0 and different relative humidities. Dry surface efficiency is also estimated from the present analysis by putting zero value of latent heat of condensation. For the comparative study, efficiency predicted by previous authors [14] is also furnished in this figure. Again present results coincide with the previous result [8] whereas a difference in efficiency is noticed when it is compared between present and Sharqawy and Zubair [14] results. This difference in results for fully wet fins increases with the relative humidity and maximum difference is found for the 100% relative humidity. The temperature distribution determined by Sharqawy and Zubair [14] is always higher than the actual value as a result the prediction of fin efficiency by using Sharqawy and Zubair analysis [14] gives lower value as shown in Fig. 7. Thus from the illustration, it is undoubtedly mentioned that the efficiency determined by the previous study [14] is always an under predict until a case when the actual tip temperature is equal to the dew point temperature. The variation of fin efficiency for wet step fins with fin parameter Z_0 is shown in Fig. 8. Like

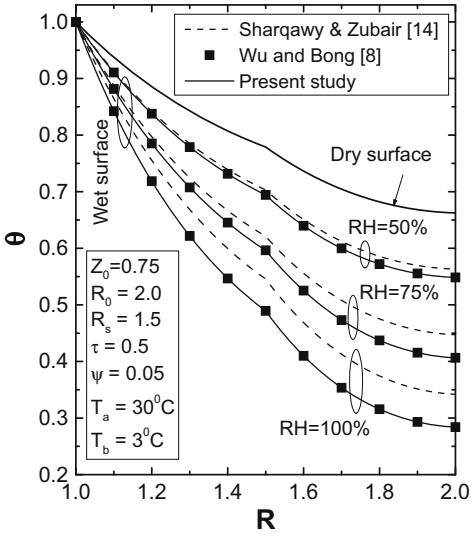

Fig. 5. Variation of dimensionless temperature distribution with the radial distance for an AFST under both the dry and wet surface conditions.

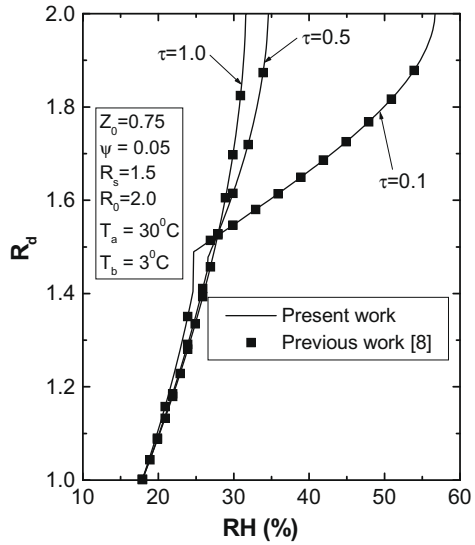

Fig. 6. Radial wet lengths of ASFs as a function of relative humidity under dehumidifying conditions.

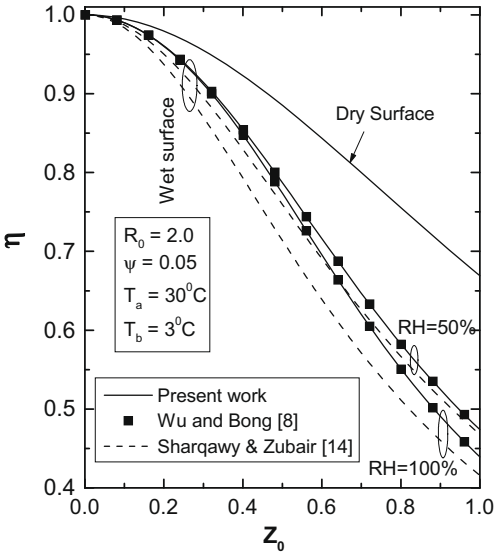

Fig. 7. Fin efficiency of annular disc fins as function of Z_0 under both dry and wet conditions estimated by present and published models.

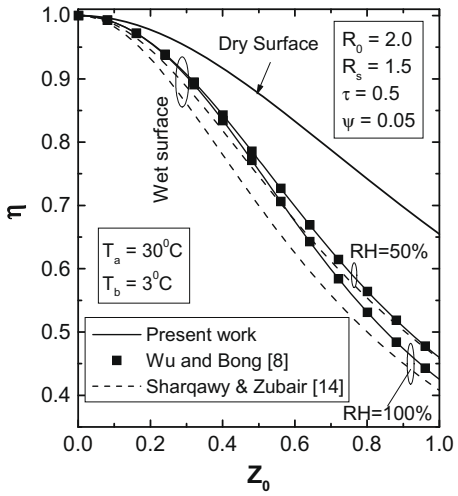

Fig. 8. Fin efficiency of ASFs as function of Z_0 under both dry and wet conditions estimated by present and published models.

annular disc fin, a same nature in curve is found for an ASF. However, the value of fin efficiency for the ASF is always smaller while it is compared with that for the annular disc fin.

Next in order to establish the merit of the present work, an exercise has been devoted for the comparison of fin efficiency calculated by the present and previous analyses for the whole range of relative humidity. Fig. 9 is drawn for the aforementioned purpose. From the figure, it is clear that there is no deviation of result predicted by different methods of analysis up to a relative humidity to initiate the fully wet surface. With the further increase in relative humidity, prediction of efficiency by different analyses shows different values as shown in Fig. 9. Once again, Wu and Bong results [8] coincide with the present result for the whole range of relative humidity whereas the prediction of results differs when a comparison is made with the results of Sharqawy and Zubair model [14] in the fully wet zone and also it can be demonstrated that this departure of fin efficiency increases gradually with the increasing relative humidity. Thus for the analysis of fully wet fins with higher values of relative humidity, the fin efficiency estimated with considering dew point temperature at the tip gives an erroneous result.

The geometrical parameters τ and R_s of step fins create a difference from a constant thickness fin. The effect of these geometrical parameters on the fin efficiency under different surface conditions is depicted in Fig. 10. With the variation of τ on the fin efficiency

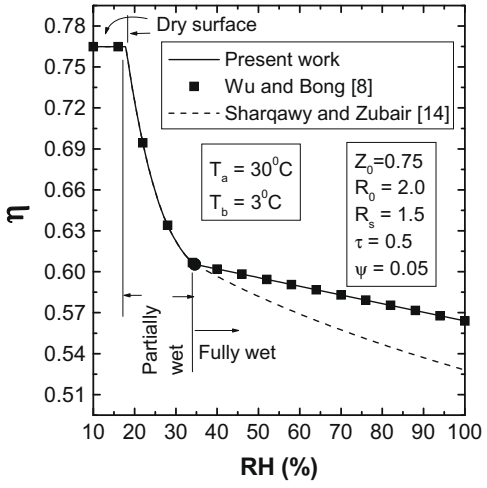

Fig. 9. Fin efficiency of ASFs as function of relative humidity under both dry and wet conditions estimated by present and published models.

for an ASF, Fig. 9a is plotted by taking $R_s = 1.5$. From this figure, it is clearly understandable that the fin efficiency is a strong function on the geometric parameter τ irrespective of the surface condition. With the increase in geometric parameter τ, fin efficiency increases continuously and a maximum efficiency is shown for $\tau = 1$ under any designed condition. In this point of view, it can be mentioned that for $\tau = 1$, ASF converts into an annular disc fin and thus the efficiency for annular disc fin is always higher than that for the ASF. Form the Fig. 10a, it can also be highlighted that for the partially wet surface, the length of the wet part increases with the increase in τ for constant relative humidity. Therefore, it can be demonstrated that whether a surface becomes fully or partially wet, the geometrical parameter τ is also important. Fig. 10b depicts the variation of fin efficiency with the dimensionless distance R_s at which step change in thickness occurs. Again, the effect of R_s on the fin efficiency is executed as a similar in nature with that of the variation of τ. With the increase in R_s or τ, the tip temperature decreases and as a result temperature variation between fin-tip and fin-base decreases which affects to increase the fin efficiency. The effect of relative humidity on the fin efficiency can be shown in Fig. 10 and it is shown a marginal variation.

Based on the present optimization study, results have been taken for a given *Bi*. The present optimization study is equally suitable for the annular disc fin for only adaptation of the geometrical parameter $\tau = 1$. With considering this, a result of heat transfer rate of an annular disc fin is furnished with the variation of R_0 for a constant *U* and *Bi* under different wet surface conditions as shown in Fig. 11. For a comparison, this result for an annular disc fin obtained from the Sharqawy and Zubair analysis [14] are also drawn in the same figure and a difference in results has been noticed. The analysis was presented by Sharqawy and Zubair [14] with considering dew point temperature as a tip temperate for the fully wet fin for calculating only pshchrometric properties and for this reason the parameters θ_p, *B* and ξ are explicitly connected with the psychrometric properties of air. However, for the determination of temperature profile in the present study with satisfying a convective tip condition only, the actual tip temperature is not equal to the dew point temperature. In this case, an iteration scheme has been implemented to determine tip temperature in order to calculate θ_p, *B* and ξ. Again the tip temperature is a function of the geometrical parameters and thus these psychrometric variables are also function of these parameters. Using this concept, present optimization scheme is established. For a constant relative humidity curve, a well defined maximum heat transfer rate is noticed. From the heat transfer rate point of view, the published result [14] is always an under predict. However, difference in results is also dependent upon the value of R_0 and relative humidity. The maximum difference is found at the optimum condition for 100% relative humidity as shown in Fig. 11. For a constant relative humidity, variation of R_0 may affect the surface conditions of a fin. For the relative humidity 75% and 50%, a partially wet surface is obtained for the outer radius which is larger than the positions A and B, respectively. From the optimum curves CEG for the present analysis and CDF for the published analysis, CE and CD represent the partially condition and, EG and DF represent the fully wet surface. Thus it can be demonstrated that for a wide range of thermo-psychrometric parameters, a fully wet surface condition is found at the optimum point. Therefore, it is to mention that the attention can be given more for the optimum design of fully wet fins instead of partially one. From the optimization study, it is worthy to mention that the optimum outer radius R_0 for a wet fin decreases with the increase in relative humidity for a constant fin volume. However, this decreased rate is more pronounced for the partially wet surface condition. A similar exercise has also been made for an ASF (Fig. 11b) with $\tau = 0.5$ and $R_s = 1.5$ chosen

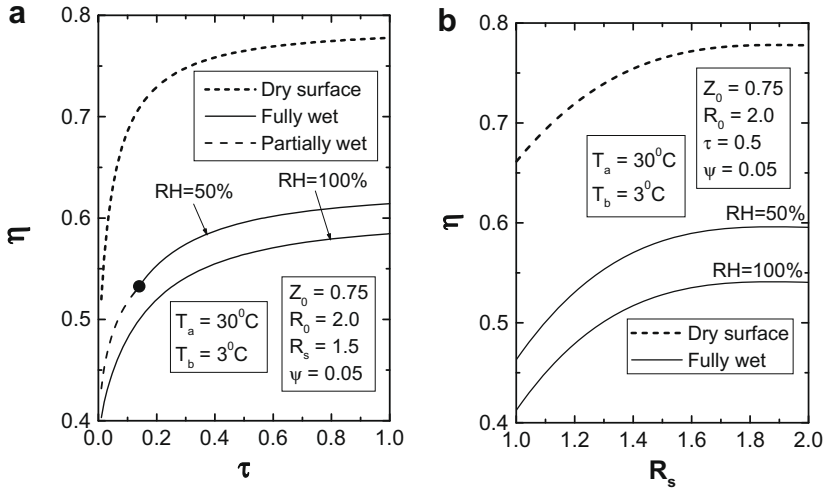

Fig. 10. Fin efficiency of ASFs as a function of geometrical parameters τ and R_s under both dry and wet conditions: (a) η vs τ; (b) η vs R_s.

arbitrarily. For the step fin, optimization study has also been done with a method followed by the analysis of published work [14] and in comparison; this result is also plotted in the same figure.

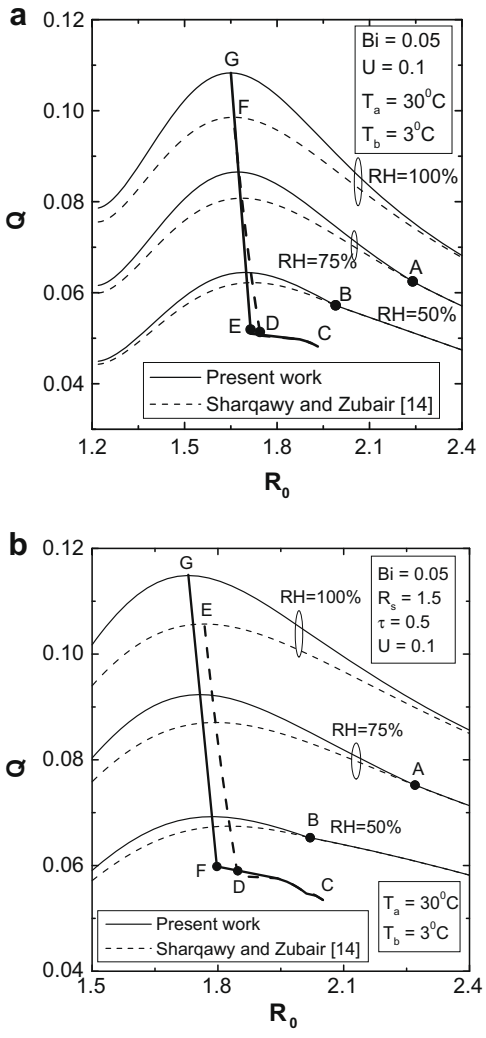

Fig. 11. Heat transfer rate as a function of radius ratio R_0 for different relative humidities: (a) annular disc fin and (b) ASF.

The same order of difference in results has been executed as already displayed in the case of annular disc fin.

Next the effect of ambient temperature on the maximum heat transfer rate for both the annular disc and ASF has been studied. For this, an optimization scheme is developed with the variation of ambient temperature and results are generated by using the present and published analyses. With the variation of ambient temperature, the maximum heat transfer rate from the present and published works for both the annular disc fin and ASF are plotted, separately as shown in Fig. 12. An increase in ambient temperature for a fixed base temperature affects to increase the maximum heat transfer rate for both the fins but the difference in results with the ambient temperature from the present and published analyses [14] is an incremental function. Therefore, the error in results with considering the tip temperature as a dew point temperature can be minimized for a lower value of ambient temperature. With the increase in ambient temperature, a partially wet surface is converted into the fully wet surface. For a comparative study of maximum heat transfer rate through the annular disc fin and that of the step fin, Fig. 12c is plotted under a design condition. A higher heat transfer rate is obtained through step fins instead of annular disc fins. However, difference in results is almost a constant with the variation of ambient temperature for a constant relative humidity. Moreover, this difference increases with the increasing relative humidity.

The atmospheric pressure depends on the position of the place with respect to the height from the mean see level. For example, a position of a hilly area is always higher than the mean sea level because of that atmospheric pressure at the hilly area is lower in comparison with the standard value. On the other hand, fin-base temperature depends on the application in which fin is used. So the knowledge of the variation of these two parameters on the fin heat transfer characteristics is also essential to a designer. The effect of atmospheric pressure and base temperature on the maximum transfer of heat rate of an ASF for $Bi = 0.05$, $\tau = 0.5$, $R_s = 1.5$, $T_a = 30$ °C and $U = 0.1$ are investigated by the present and previous methods which is depicted in Fig. 13. From the figure, it is clear that for the range of psychrometric parameters taken, fin surface of ASFs satisfies a fully wet condition and an increase in atmospheric pressure decreases the heat transfer rate. With the increase in atmospheric pressure, rate of condensation on the fin surface decreases as a result declines the heat transfer rate. Nevertheless, this effect is varied at a slower rate. The variation of fin-base temperature on the optimum transfer of heat rate is shown in Fig. 13b. In

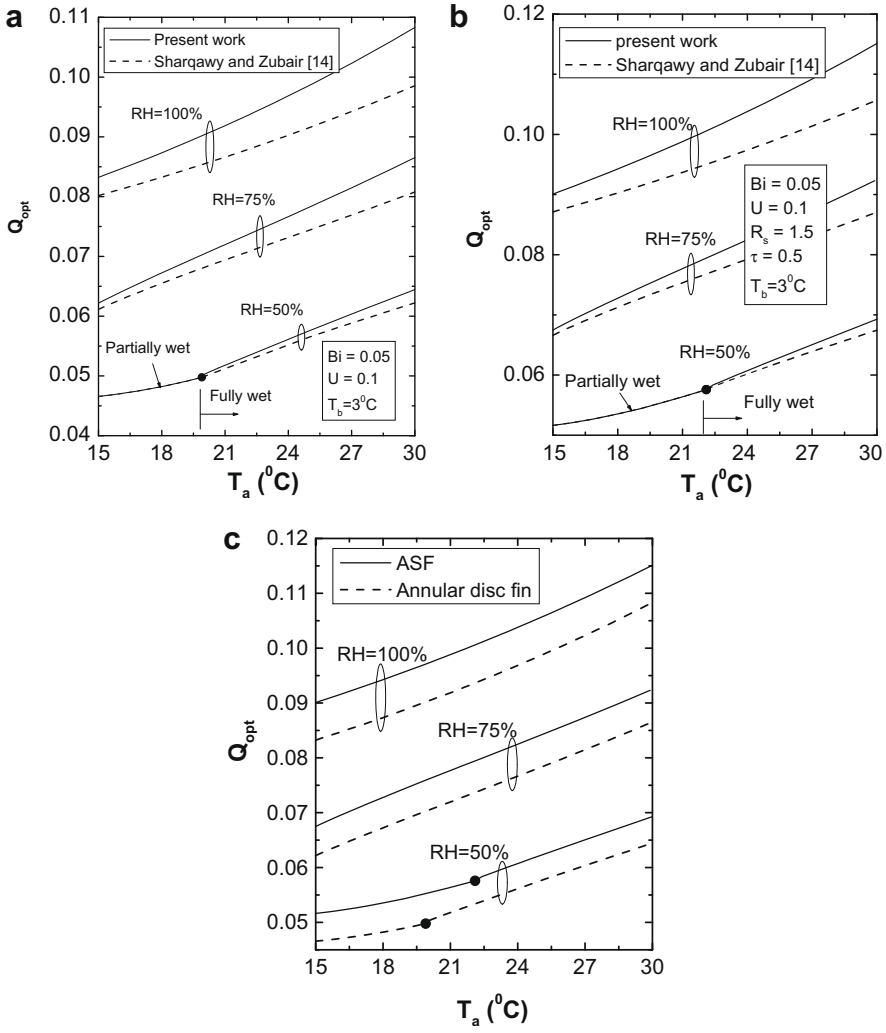

Fig. 12. Maximum heat transfer rate as a function of relative humidity and ambient temperature: (a) present and published results of annular fins, (b) present and published results of ASFs, and (c) comparison in heat transfer rate between annular fins and ASFs.

the case of the relative humidity of 100%, maximum transfer of heat increases with the increase in base temperature. A reverse effect is noticed for the relative humidity of 70% and 50% with the base temperature. Actually with the increase in fin-base temperature, both the sensible and latent heat rate decreases. The variable Q is a normalized heat transfer rate which is also function of the fin-base temperature T_b for a constant ambient temperature. Thus although the dimensional rate of heat decreases with the fin-base temperature, the dimensionless heat rate may increase for a constant relative humidity.

4. Conclusions

Dehumidification of air on the fin surface takes place when the fin surface temperature is below the dew point temperature. For the analysis of heat and mass transfer mechanisms, the variation of the specific humidity of air with the corresponding temperature follows with a psychrometric relationship and in the case of refrigeration and air conditioning applications, this relation can be taken as a linear one for the small range of temperature existed between fin-base and fin-tip. In the present study, the specific humidity of air on the fin surface varies owing to the variation of fin temperature and it is determined by using the fin-base and fin-tip temperatures with a linear relationship. No previous works have so far been clearly indicated for the determination of fin surface temperature for the fully wet fins with considering the actual tip condition. The actual tip temperature has been found by solving the energy equation with appropriate boundary conditions. For the solution, it is needed the psychrometric properties of air which is also dependent upon the tip temperature. In lieu of that, Sharqawy and Zubair [14] have chosen tip temperature as a dew point temperature for calculating the psychrometric parameters. In actual case psychrometric parameters depend also on the actual tip temperature which may not be equal to the dew point temperature. In the present work for the fully wet fin, a guess tip temperature is assumed initially for determining psychrometric properties of air and then they are substituted in the expression of temperature in order to calculate the actual tip temperature. The process is repeated until the difference between present and just previous tip temperatures is a very small value. Finally, the actual tip temperature and temperature distribution are obtained.

Due to the gradual decrease in heat conduction rate from the fin-base to fin-tip, effective utilization of fin material may not be possible for annular disc fins. For this reason, different tapered fins had already been investigated by many researchers. However, among of these a very few one is compatible in manufacturing process. Because of that annular disc fin is extensively found in various applications. Lot of investigations is still engaged to modify the geometry of the annular disc fin on the basis of enhancement of heat transfer rate as well as ease of fabrication. Based on these cri-

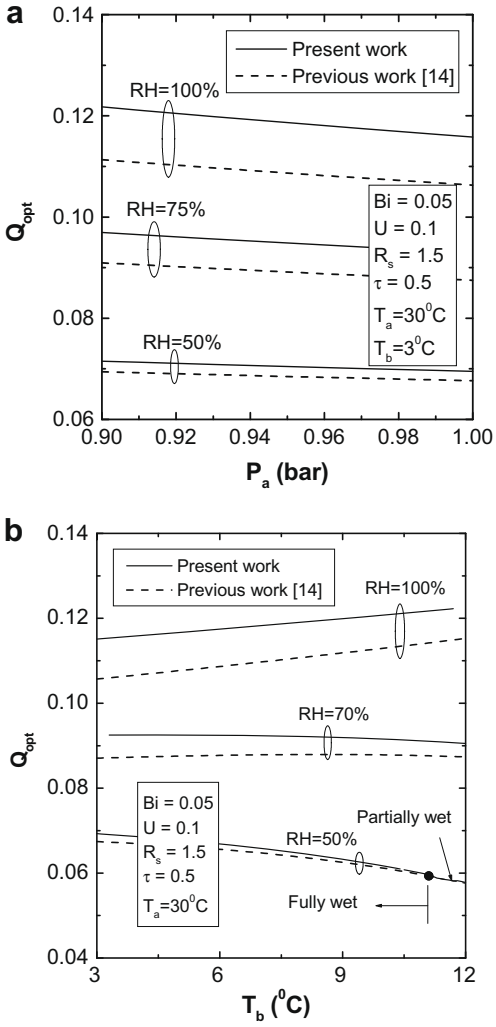

Fig. 13. Variation of atmospheric pressure and base temperature on the optimum heat transfer rate for an ASF under wet conditions: (a) Q_{opt} vs P_a, (b) Q_{opt} vs T_b.

teria, ASF is one of the suitable geometry. The present work is concentrated on the performance and optimization analysis of ASFs under wet surface conditions. From the above discussions, the following conclusions can be drawn:

1. Dehumidification of air depends not only on the psychrometric condition of air on the fin surface but also on the surface temperature of the fin.
2. Fin surface temperature for wet fins is an implicit function with the thermo-physical, psychrometric and geometric parameters.
3. For a practical range of design parameters, there is a very high chance to obtain a fully wet surface instead of a partially wet fin.
4. With the relative humidity for the fully wet fin, the error of results associated with considering the tip temperature as a dew point temperature for calculating the psychrometric parameters is an increasing function.
5. The overall efficiency of ASFs under wet conditions increases with the increase in both the geometrical parameters τ and R_s.
6. The optimality criteria for annular fins are established in a generalized way such that either the rate of heat transfer or the fin volume can be taken as a constant. According to the requirement of a design, any modification can be done easily to determine the optimum condition.
7. The optimum geometrical parameters determined by using the present study are also an implicit function with the psychrometric parameters. However, in the previous studies, these were treated explicitly.
8. With considering dew point temperature as a tip temperature for calculating psychrometric parameters, heat transfer rate is always lower than that of the actual tip temperature under the condition of fully wet surface. However, a maximum difference is noticed at the optimum point for the 100% relative humidity.
9. Increase in ambient temperature increases the optimum heat transfer rate for the fully as well as partially wet fins.
10. Increasing both the ambient pressure and fin-base temperature decrease the rate of heat transfer for any wet fin.
11. The optimum ASF transfers more rate of heat in comparison with that of the annular disc fin for the same thermo-physical and psychrometric parameters.
12. The present analysis is equally suitable for the dry surface condition also with the consideration of zero value of the latent heat of condensation.
13. The present analysis of ASF is equally suitable for the analysis of annular disc fins only consideration of the geometrical parameter $\tau = 1$.

References

[1] J.L. Threlkeld, Thermal Environmental Engineering, Englewood Cliffs, NJ, 1970.
[2] ARI Standard 410-72, Forced-Circulation Air-Cooling and Air-Heating Coils, Air-Conditioning & Refrigeration Institute, 1972.
[3] F.C. McQuiston, Fin efficiency with combined heat and mass transfer, ASHRAE Trans. 81 (1975) 350–355.
[4] J.E.R. Coney, C.G.W. Sheppard, E.A.M. El-Shafei, Fin performance with condensation from humid air: a numerical study, Int. J. Heat Fluid Flow 10 (1989) 224–231.
[5] J.E.R. Coney, H. Kazeminejad, C.G.W. Sheppard, Dehumidification of air on a vertical rectangular fin: a numerical study, Proc. Inst. Mech. Eng. 203 (1989) 141–146.
[6] A. Kilic, K. Onat, The optimum shape for convecting rectangular fins when condensation occurs, Wame Stoffubertragung 15 (1981) 125–133.
[7] V. Srinivasan, R.K. Shah, Fin efficiency of extended surfaces in two-phase flow, Int. J. Heat Fluid Flow 18 (1997) 419–429.
[8] G. Wu, T.Y. Bong, Overall efficiency of a straight fin with combined heat and mass transfer, ASHRAE Trans. 100 (1994) 367–374.
[9] H. Kazeminejad, Analysis of one-dimensional fin assembly heat transfer with dehumidification, Int. J. Heat Mass Transfer 38 (1995) 455–462.
[10] A.H. Elmahdy, R.C. Biggs, Efficiency of extended surfaces with simultaneous heat and mass transfer, ASHRAE Trans. 89 (1983) 135–143.
[11] K.T. Hong, R.L. Webb, Calculation of fin efficiency for wet and dry fins, HVAC&R Res. 2 (1996) 27–40.
[12] L. Rosario, M.M. Rahman, Overall efficiency of a radial fin assembly under dehumidifying conditions, J. Energy Resources Technol. 120 (1998) 299–304.
[13] P. Naphon, Study on the heat transfer characteristics of the annular fin under dry-surface, partially wet-surface, and fully-wet surface conditions, Int. Commun. Heat Mass Transfer 33 (2006) 112–121.
[14] M.H. Sharqawy, S.M. Zubair, Efficiency and optimization of an annular fin with combined heat and mass transfer – an analytical solution, Int. J. Refrig. 30 (2007) 751–757.
[15] M.H. Sharqawy, S.M. Zubair, Combined heat and mass transfer analysis from annular fins of constant cross-sectional area, in: 8th International Symposium on Advances in Computational Heat Transfer Proceedings, ICHMT, Marrakech, Morocco, Paper# CHT-08-239, May 2008.
[16] C.C. Wang, Y.C. Hsieh, Y.T. Lin, Performance of plate finned tube heat exchangers under dehumidifying conditions, J. Heat Transfer 119 (1997) 109–117.
[17] R.K. Shah, in: W.M. Rohsenow, J.P. Hartnett, E.N. Ganic (Eds.), Compact Heat Exchanger, in Handbook Heat Transfer Applications, second ed., McGraw Hill, New York, 1985.
[18] C.C. Wang, A tube-by-tube reduction method for simultaneous heat and mass transfer characteristics for plain fin-and-tube heat exchangers in dehumidifying conditions, Heat Mass Transfer 41 (2005) 756–765.
[19] W. Pirompugd, C.C. Wang, S. Wongwises, Finite circular fin method for heat and mass transfer characteristics for plain fin-and-tube heat exchangers under fully and partially wet surface conditions, Int. J. Heat Mass Transfer 50 (2007) 552–565.

[20] J.Y. Jang, C.N. Lin, Two-dimensional fin efficiency of plate fin-tube heat exchangers under partially and fully wet conditions, J. Thermal Sci. 11 (2002) 249–254.
[21] A. Hasan, K. Siren, Performance investigation of plain and finned tube evaporatively cooled heat exchangers, Appl. Thermal Eng. 23 (2003) 325–340.
[22] C.N. Lin, J.Y. Jang, A two-dimensional fin efficiency analysis of combined heat and mass transfer in elliptic fins, Int. J. Heat Mass Transfer 45 (2002) 3839–3847.
[23] H. Kazeminejad, M.A. Yaghoubi, M. Sepehri, Effect of dehumidification of air on the performance of eccentric circular fins, Proc. Inst. Mech. Eng. 207 (1992) 141–146.
[24] A. Toner, K. Killic, K. Onat, Comparison of rectangular and triangular fins when condensation occurs, Wame Stoffubertragung 17 (1983) 65–72.
[25] B. Kundu, An analytical study of the effect of dehumidification of air on the performance and optimization of straight tapered fins, Int. Commun. Heat Mass Transfer 29 (2002) 269–278.
[26] B. Kundu, P.K. Das, Performance and optimization analysis for fins of straight taper with simultaneous heat and mass transfer, ASME J. Heat Transfer 126 (2004) 862–868.
[27] B. Kundu, Optimization of fins under wet conditions using variational principle, J. Thermophys. Heat Transfer 22 (4) (2008) 604–616.
[28] B. Kundu, P.K. Das, Performance analysis and optimization of annular fin with a step change in thickness, J. Heat Transfer 123 (2001) 601–604.
[29] T.H. Chilton, A.P. Colburn, Mass transfer (absorption) coefficients, Ind. Eng. Chem. 26 (1934) 1183–1187.
[30] M.M. El-Din Sala, Performance analysis of partially wet fin assembly, Appl. Thermal Eng. 18 (1998) 337–349.
[31] J.B. Scarborough, Numerical Mathematical Analysis, Oxford & IBH, New Delhi, 1966.
[32] W.F. Stoecker, Design of Thermal System, third ed., McGraw Hill, New York, 1989.